




## Article – Frank Reith memorial issue

# Toxicity assessment of gold ions and gold nanoparticles to golden perch larvae (*Macquaria ambigua*)

Jeremiah Shuster<sup>1,2\*</sup> , Maria A.D. Rea<sup>2,3</sup>, Bhanu Nidumolu<sup>2</sup> and Anupama Kumar<sup>2</sup>

<sup>1</sup>The University of Adelaide, School of Biological Sciences, North Terrace, Adelaide, South Australia 5005, Australia; <sup>2</sup>Commonwealth Scientific and Industry Research Organization: Land and Water, Environmental Protection and Technologies Team, Waite Road PMB2, Urrbrae, South Australia 5064, Australia; and <sup>3</sup>Flinders University, College of Science and Engineering, Sturt Road, Bedford Park, South Australia 5042, Australia

### Abstract

Golden perch (*Macquaria ambigua*) is a freshwater game-fish native to central and southeast Australia. Larvae of this fish species were used in two different types of experiments to evaluate the effects of short-term exposures (up to 6 days) to aqueous gold, 5 nm gold nanoparticles (AuNPs), or 50 nm AuNPs. Relative to the control, increased gold concentrations corresponded with yolk-sac edema (swelling). Larvae exposed to 50 µM of 5 nm AuNPs had yolk-sacs that were ~1.5 times larger resulting in the appearance of bent notochords. After two days of exposure, 100% mortality was observed. Total mortalities were <25% in the other larvae–gold systems, suggesting that these larvae can quickly adapt to the presence of gold. In terms of an oxidative stress response, the larvae from all systems did not express high enzymatic activity. The state of the gold determined how much could be taken up (or immobilised) by a larva. Aqueous gold and 5 nm AuNPs easily pass through cells; therefore, larvae exposed to these forms of gold contained the highest concentrations. Scanning electron microscopy confirmed that cells comprising the epithelium and fins contained AuNPs. Aqueous gold was reduced to nanometre-scale particles within cells. Comparatively, 5 nm AuNPs appeared to be aggregated within cells forming clusters hundreds of nanometres in size. On the contrary, 50 nm AuNPs were not observed within cells but were detected within larvae by (single particle) inductively coupled plasma mass spectroscopy, suggesting that these AuNPs were probably taken up through the mouth or gills. The results of the present study demonstrate that exposure to AuNPs had adverse effects on developing golden perch larvae. Additionally, these effects were dependent on the size of the AuNPs.

**Keywords:** golden perch, oxidative stress, gold nanoparticles, gold, biomineralisation

(Received 13 January 2021; accepted 3 February 2021; Accepted Manuscript published online: 8 February 2021; Guest Associate Editor: Janice Kenney)

### Preface

This publication was written to commemorate the late Associate Professor Frank Reith – our colleague, mentor and friend. Frank's research focused primarily on understanding the interactions between bacteria and gold; however, he strove to diversify and expand gold biogeochemistry research. In 2006, Frank joined the Commonwealth Scientific and Industry Research Organization (CSIRO) and his research group (Microbes and Heavy Metal) remained integrated at the CSIRO Waite Campus (Urrbrae, South Australia). After working alongside Dr Anupama Kumar for nearly a decade at CSIRO, they developed a collaborative research project that bridged the disciplines of gold biogeochemistry with ecotoxicology. In doing so, members of the Microbe and Heavy Metal and CSIRO's Environmental Contaminant Mitigations and Biotechnologies Programme collaborated. Together, these groups brought this study to fruition despite Frank's lamentable absence. While this study is fundamental in its outcomes, it highlights the potential for developing further

interdisciplinary collaborations to address issues related to ecotoxicology and assessing the impact of anthropogenic activity on natural environments.

### Introduction

In natural environments, gold nanoparticles (AuNPs) are associated with clay minerals on the surface of placer gold particles. Some of these AuNPs appear semi-spherical but are actually euhedral crystals ranging from 10s to 100s of nm in size and contribute to secondary gold enrichment on the surface of particles (Reith *et al.*, 2013 and references therein; Shuster *et al.*, 2017). On the contrary, synthesised AuNPs are colloidal and ≤100 nm in size. The first evidence of AuNPs applications date back to 'ancient' Arabia, China and India where colloidal solutions were used as medicinal elixirs. During the Middle Ages in Europe, the use of colloidal solutions as treatments for a variety of illnesses continued. For example, King Louis XIII of France was given a colloidal gold solution as an elixir for longevity by the alchemist David de Planis-Campy (Dykman and Khlebtsov, 2011). It was not until the 1970s when AuNPs were used in practical biomedical applications; specifically imaging antigens on the surface of *Salmonellae* sp. using electron microscopy (Dykman and Khlebtsov, 2011). Since then, the use of AuNPs in biomedical

\*Author for correspondence: Jeremiah Shuster, Email: [jeremiah.shuster@adelaide.edu.au](mailto:jeremiah.shuster@adelaide.edu.au)  
This paper is part of a thematic set in memory of Frank Reith  
Cite this article: Shuster J., Rea M.A.D., Nidumolu B. and Kumar A. (2021) Toxicity assessment of gold ions and gold nanoparticles to golden perch larvae (*Macquaria ambigua*). *Mineralogical Magazine* 85, 94–104. <https://doi.org/10.1180/mgm.2021.14>

application has diversified (e.g. clinical chemistry to targeted drug delivery) and has been also used in electronic as well as cosmetic applications (Chen *et al.*, 2014; Bhagyaraj and Oluwafemi, 2018). As the number of applications involving AuNPs continues to increase, it is reasonably foreseeable that some AuNPs could inadvertently contaminate natural environments. The need to assess the potential impacts of precious metals on the environment has already been highlighted by the use of silver nanoparticles in commercial products (i.e. Khaksar *et al.*, 2015). Synthetic AuNPs could enter aquatic environments directly from industrial manufacturing or from waste materials. In aquatic environments, various plants, crustaceans, or fish could potentially come in contact with AuNPs. Previous studies have investigated how short-term nanoparticle exposures affect organ development or cause mortality (acute toxicity) in a variety of organisms (Alkilany and Murphy, 2010). Fish are sensitive to environmental stressors especially during early development (i.e. larval stage). For example, physiological defects during the larvae stage could potentially impair reproduction once the fish has reached maturity thereby impacting on fish populations. Golden perch (*Macquaria ambigua*) is a type of freshwater fish that is native from central to southeast Australia and is often used in recreational sport fishing (Carragher and Rees, 1994). Golden perch spawn during the spring or summer and the fecundity of a mature golden perch can be up to 500,000 eggs. Fertilised eggs are 3–4 mm in diameter, colourless and semi-buoyant. Larvae emerge after 24 h and have a yolk-sac. Larvae start feeding 6–7 days post-hatch and are fully developed after 18–20 days. Although growth can be variable, full maturity in males and females is reached at 3–4 and 6 years old, respectively, and adult fish can reach up to 50 cm in length (Reynolds 1983; Mallen-Copper *et al.*, 1995; Harris and Rowland, 1996). The presence of dams has inhibited the migration of adult fish to spawning grounds, which has led to decreased populations or resulted in complete disappearance in some regions. Therefore, golden perch was listed as a vulnerable species under the Victorian Flora and Fauna Guarantee Act 1988. To date, there is paucity of research on the effects of gold (aqueous or nanoparticulate) on golden perch larvae. Based on the above information, the following hypotheses were tested: exposure to gold nanoparticles does not result in adverse effects in golden perch larvae (null hypothesis), exposure to gold nanoparticles results in adverse effects such as abnormalities in golden perch larvae (alternate hypothesis I), the severity of effects depends upon the size of gold nanoparticles (alternate hypothesis II). Overall, the aim of this project was to determine the effect of short-term exposures to different concentrations and different size AuNPs on golden perch larvae under controlled laboratory conditions.

## Materials and methods

### *Fish larvae and sources of gold*

One-day old golden perch larvae were purchased from a fisheries station (Narrendera, NSW Australia) and assessed for physical abnormalities before experimental use. No abnormalities were observed. Pure ( $\geq 99.9\%$ ) gold chloride ( $\text{AuCl}_3$ ) was purchased from Alfa Aesar (Victoria, Australia). A measured  $5\ \mu\text{M}$  gold stock solution was prepared by dissolving gold chloride into deionised water. The gold stock solution was twice filter-sterilised using  $0.1\ \mu\text{m}$  pore-size filters and stored in a sealed Schott bottle wrapped in aluminium foil to prevent photocatalytic reduction of gold. Pure gold nanoparticles (AuNPs with 5 or 50 nm diameters)

suspended in deionised water were purchased from Nanopartz Inc. (Colorado, USA). Prior to experimental use, the vials were placed in a PowerSonic Ultrasonic water bath for  $\sim 10$  s to ensure that the AuNPs were dispersed in solution.

### *Experiments: fish larvae–gold systems*

All experiments were based on the Organisation for Economic Co-operation and Development guidelines (1998) Test No. 212: Fish, short-term toxicity test on embryo and sac-fry stages and conducted under CSIRO Animal Ethics Committee Project Number 817. Two types of experiments were constructed using sterile borosilicate glass beakers containing fish larvae in 50 mL of deionised water ( $\text{pH } 7.7 \pm 0.3$ ) and gold. Experiment I involved the exposure of 10 fish larvae to  $0.05\ \mu\text{M}$  gold. In these fish larvae–gold systems, gold occurred as either aqueous gold ( $\text{AuCl}_3$ ), 5 nm AuNPs, or 50 nm AuNPs. In Experiment II, fish larvae were exposed to higher concentrations (5 or  $50\ \mu\text{M}$ ) of 5 or 50 nm AuNPs. A control containing 10 larvae and 50 mL deionised water was performed in parallel with Experiments I and II. All fish larvae–gold systems and controls were incubated in a 16 h light/8 h dark cycle incubator for six days at  $23 \pm 2^\circ\text{C}$ . Each concentration included four replicates (beakers). During semi-static exposure, solutions were replaced every 24 hrs. Dissolved oxygen and pH of all systems were monitored using a CyberScan multi-meter with pH calibrated to 4.0, 7.0 and 10.0 reference standards. Any morphological changes or deceased fish larvae were recorded. During the exposure period, deceased fish larvae were removed from the respective beakers to avoid contamination. These larvae were individually placed in 1 mL-volume Eppendorf tubes containing deionised water, and were snap frozen using liquid nitrogen. After seven days of incubation, all remaining larvae were individually snap frozen.

Ten snap-frozen larvae, selected randomly from each larvae–gold system and control, were transferred to  $10\%_{(\text{aq})}$  formalin for at least 24 hours to defrost whilst preserving their cellular structure. These ‘fixed’ larvae were imaged using an Olympus SZX9 stereomicroscope equipped with an Olympus SC180 digital camera and Olympus LG-PS2 light source. Yolk-sac width and height were measured using the Olympus Image Analysis Software and known pixel dimensions. The larvae were kept in formalin for preparation for scanning electron microscopy analysis (described below).

### *Enzymatic activity analysis*

To assess the stress response of larvae exposed to gold, enzyme (catalase, glutathione reductase and glutathione S-transferase) activity assays were performed. From each larvae–gold system and control, five larvae were selected randomly and pooled to represent each system. Pooled larvae were placed in 200  $\mu\text{L}$  of 100 mM potassium phosphate buffer ( $\text{pH } 7.0$ ) and pulverised using a bead beater to homogenise the sample. The homogenised samples were centrifuged (14,000 rpm for 15 minutes at  $4^\circ\text{C}$ ) and the supernatants (i.e. enzyme extract) were collected. Total protein content of the enzyme extracts was estimated according to method defined by Bradford (1976) using bovine serum albumin (Sigma Aldrich) as a standard.

Catalase (CAT) activity was determined by hydrogen peroxide ( $\text{H}_2\text{O}_2$ ) decomposition in the method defined by Aebi (1984). In doing so, a reaction mixture was made by adding 100 mM phosphate buffer ( $\text{pH } 7.0$ ) and 20 mM  $\text{H}_2\text{O}_2$  to an aliquot of the

enzyme extract. The change in absorbance at 240 nm was measured using a Molecular Devices Spectramax 340 Microplate Reader and Spectrophotometer. Catalase activity was calculated (equation 1) using the change in absorbance over time ( $\Delta A/t$ ) with  $t=1$  minute and the extinction coefficient ( $\epsilon^{\text{mM}}$ ) for  $\text{H}_2\text{O}_2 = 43.6 \text{ M}^{-1} \text{ cm}^{-1}$ . Concentrations were then converted to  $\text{mU mg}^{-1}$  based on the estimated total amount of protein content of the enzyme extract (equation 2).

$$U \text{ mL}^{-1} = \frac{\left( \frac{\Delta A_{\text{sample}} - \Delta A_{\text{blank}}}{t \times (\text{dilution factor})} \right)}{\epsilon^{\text{mM}} \times (\text{sample volume in mL})} \quad (1)$$

$$U \text{ mg}^{-1} = \frac{U \text{ mL}^{-1} \text{ of glutathione reductase}}{\text{mg of protein in mL}^{-1} \text{ of sample}} \quad (2)$$

For the glutathione reductase (GR) assay, a modified method by Smith *et al.* (1988) was performed. A reaction mixture was made by adding phosphate buffer, 2 mM oxidised glutathione disodium salt (GSSG), 2 mM  $\beta$ -nicotinamide adenine dinucleotide phosphate (NADPH) and 3 mM 5,5-dithiobis-2-nitrobenzoic acid (DTNB) to an aliquot of the enzyme extract at 25°C. Using the same spectrophotometer, the change of absorbance at 412 nm of the reaction mixture was measured. Glutathione reductase activity was calculated (equation 1), using the change in absorbance over time ( $\Delta A/t$ ) with  $t=10$  minutes and the extinction coefficient ( $\epsilon^{\text{mM}}$ ) of 5-thio-2-nitrobenzoic acid (TNB, a by-product of the reaction mixture:  $14.15 \text{ mM}^{-1} \text{ cm}^{-1}$ ), and converted to  $\text{mU mg}^{-1}$  (equation 2).

Glutathione S transferase (GST) assay was performed in a method modified from Drotar *et al.* (1985) by adding phosphate buffer, 40 mM 1-chloro-2,4 dinitrobenzene (CDNB) and 10 mM glutathione (GSH) to an aliquot of the enzyme extract at 25°C. Using the same spectrophotometer, the change in absorbance at 340 nm was measured. The GST activity was calculated using the same equations mentioned previously with the change in absorbance over time ( $\Delta A/t$ ) with  $t=20$  minutes and the extinction coefficient ( $\epsilon^{\text{mM}}$ ) of CDNB ( $9.6 \text{ mM}^{-1} \text{ cm}^{-1}$ ).

### Inductively coupled plasma-mass spectroscopy

Four snap-frozen larvae from Experiment I, Experiment II (involving exposures to  $50 \mu\text{M}$  AuNPs), and the respective controls were selected randomly to determine the average concentration of gold within larvae. Three of the larvae replicates were individually placed in concentrated *aqua regia* (3 parts 37%<sub>(aq)</sub> HCl to 1 part 70%<sub>(aq)</sub>  $\text{HNO}_3$ ) to completely digest the larvae and AuNPs. Note that the fourth replicates were used for single-particle inductively coupled plasma mass spectroscopy (ICP-MS, described below). Gold concentrations were measured using an Agilent 5100 Synchronous Vertical Dual View ICP-MS calibrated with gold standards. The average number of AuNPs within larvae was calculated using measured gold concentrations, particle sizes (5 or 50 nm diameters) and known unit cell dimensions.

The fourth larvae replicates were used to identify any changes in AuNPs size using single-particle inductively coupled plasma mass spectroscopy (SP-ICP-MS) and a method modified from Rea *et al.* (2020). Briefly, larvae were individually digested in 30%<sub>(aq)</sub> tetramethylammonium hydroxide (TMAH) for 24 hours to dissolve the fish larvae but not the AuNPs. Samples were

diluted (1.0%<sub>(aq)</sub> final concentration) using fresh TMAH and analysed using a PerkinElmer NexION™ 350D SP-ICP-MS calibrated with gold standards. Four AuNPs solutions (20, 40, 60, or 80 nm size AuNPs, British Biocell International, UK) were also used as reference standards. All data were processed using the Nano Application Module Syngistix™ software.

### Scanning electron microscopy-energy dispersive spectroscopy

After light microscopy analysis the same formalin-fixed larvae were imaged using a scanning electron microscope (SEM) to characterise how AuNPs were associated with larvae. In doing so, fish larvae were prepared for energy dispersive spectroscopy (EDS) analysis using a method modified from Shuster *et al.* (2019). Briefly, larvae were individually and sequentially incubated in ethanol solutions (50, 75, 90%<sub>(aq)</sub> and 100%) for 15 minutes at each concentration. The larvae were transferred to a solution containing 100% ethanol and 100% hexamethyldisilazane (HMDS) with a 1:1 ratio and incubated for 30 minutes. The larvae were transferred to 100% HMDS and incubated for an additional 30 minutes; this step was repeated albeit with a 15 minutes incubation. After the final incubation, the samples were air-dried for 24 hours, placed on aluminium stubs using carbon adhesive tabs and coated with carbon (10 nm thick). The larvae were imaged using a FEI DualBeam focused ion beam (FIB) SEM equipped with an Oxford Instrument energy dispersive X-ray spectrometer (EDXS). Micrographs were taken in secondary electron (SE) and back-scatter electron (BSE) mode using 10 and 20 keV, respectively.

## Results

### Yolk-sac morphology

Overall, the presence of aqueous gold or AuNPs correlated with increased yolk-sac height and width (i.e. relative size) from larvae in both types of experiments. From Experiment I, larvae exposed to  $0.05 \mu\text{M}$  aqueous gold had yolk-sacs that were 0.03–0.12 mm bigger in width compared to larvae from the control and larvae exposed to  $0.05 \mu\text{M}$  AuNPs, respectively (Fig. 1). Larvae from Experiment II had the greatest increase in yolk-sac size; 0.86 and 0.83 mm in width and height, respectively. Compared to the control, larvae exposed to  $50 \mu\text{M}$  of 5 nm AuNPs had yolk-sacs that were ~1.5 times larger. By measuring the angle of the notochord above the yolk-sac, larvae from the control had an average  $147^\circ$  angle. Larvae exposed to  $50 \mu\text{M}$  of 5 nm AuNPs had an average  $132^\circ$  angle thereby giving them a forward bending arched shape (Fig. 1).

### Oxidative stress response

In general, fish larvae from the majority of experiments contained protein concentrations that were within the range detected from the control system across all enzyme (CAT, GR and GST) assays. Of these assays, catalase had both the greatest average protein concentrations as well as greatest range. In terms of nanoparticle size, protein concentrations were generally more variable from larvae exposed to 50 nm AuNPs relative to larvae exposed to 5 nm AuNPs.

From Experiment I, larvae exposed to  $0.05 \mu\text{M}$  aqueous Au contained average CAT, GR and GST concentrations that were 12, 7 and  $3 \text{ mU mg}^{-1}$  greater, respectively, compared to the

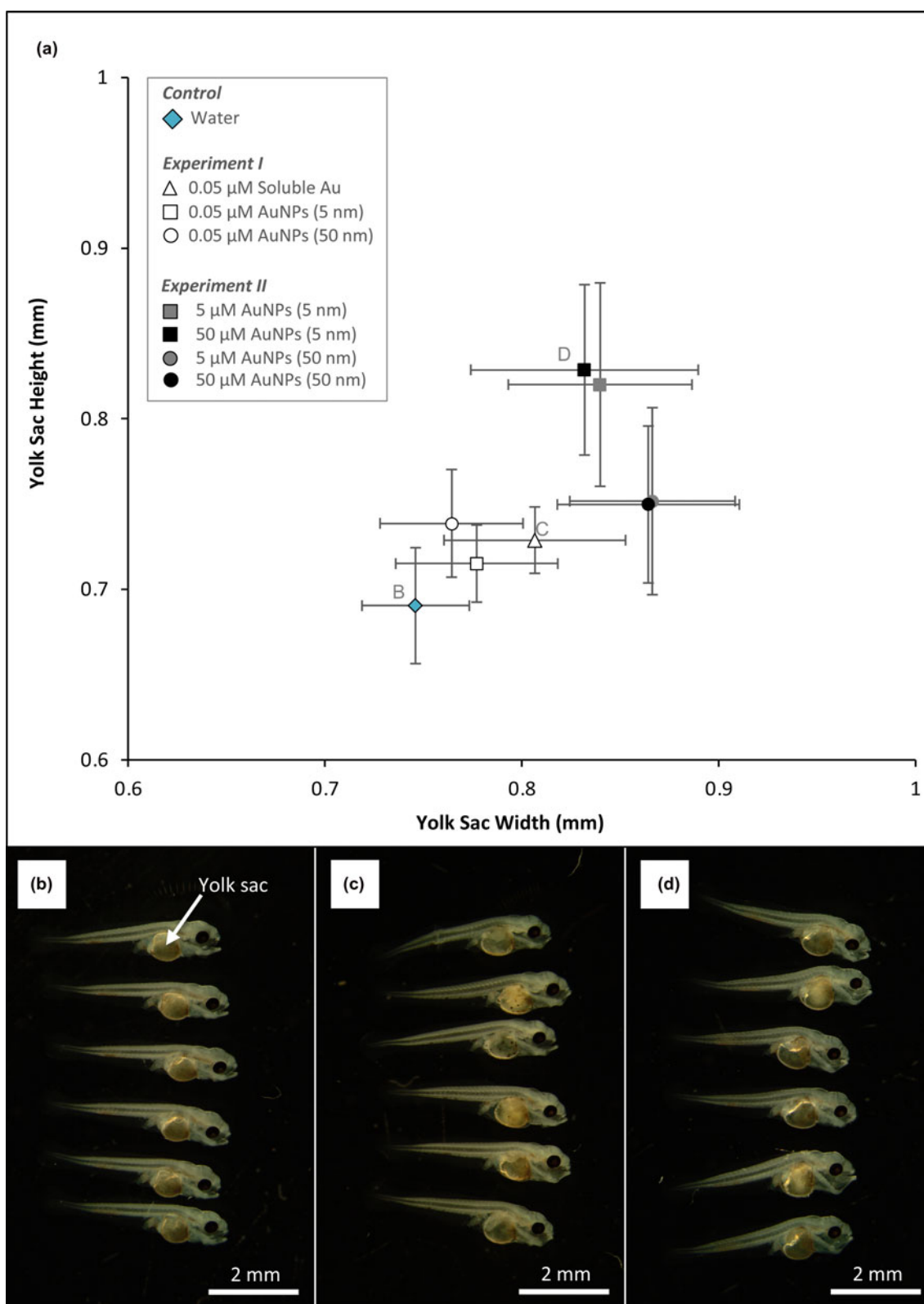


**Fig. 1.** (a) Changes in yolk-sac height and width of larvae from Experiments I and II and the control. (b) A photograph of fish larvae from the control; (c) exposed to 0.05  $\mu$ M aqueous gold for seven days; (d) exposed to 50  $\mu$ M of 5 nm size AuNPs for three days.

control. Larvae exposed to 0.05  $\mu$ M of 5 nm AuNPs had average CAT and GST and GR concentrations that were similar to the controls. Larvae exposed to 0.05  $\mu$ M of 50 nm AuNPs, however,

had an average CAT concentration that was 20  $\text{mU mg}^{-1}$  greater than the control. In this same system, the average GST concentration had little change while the average GST concentration was



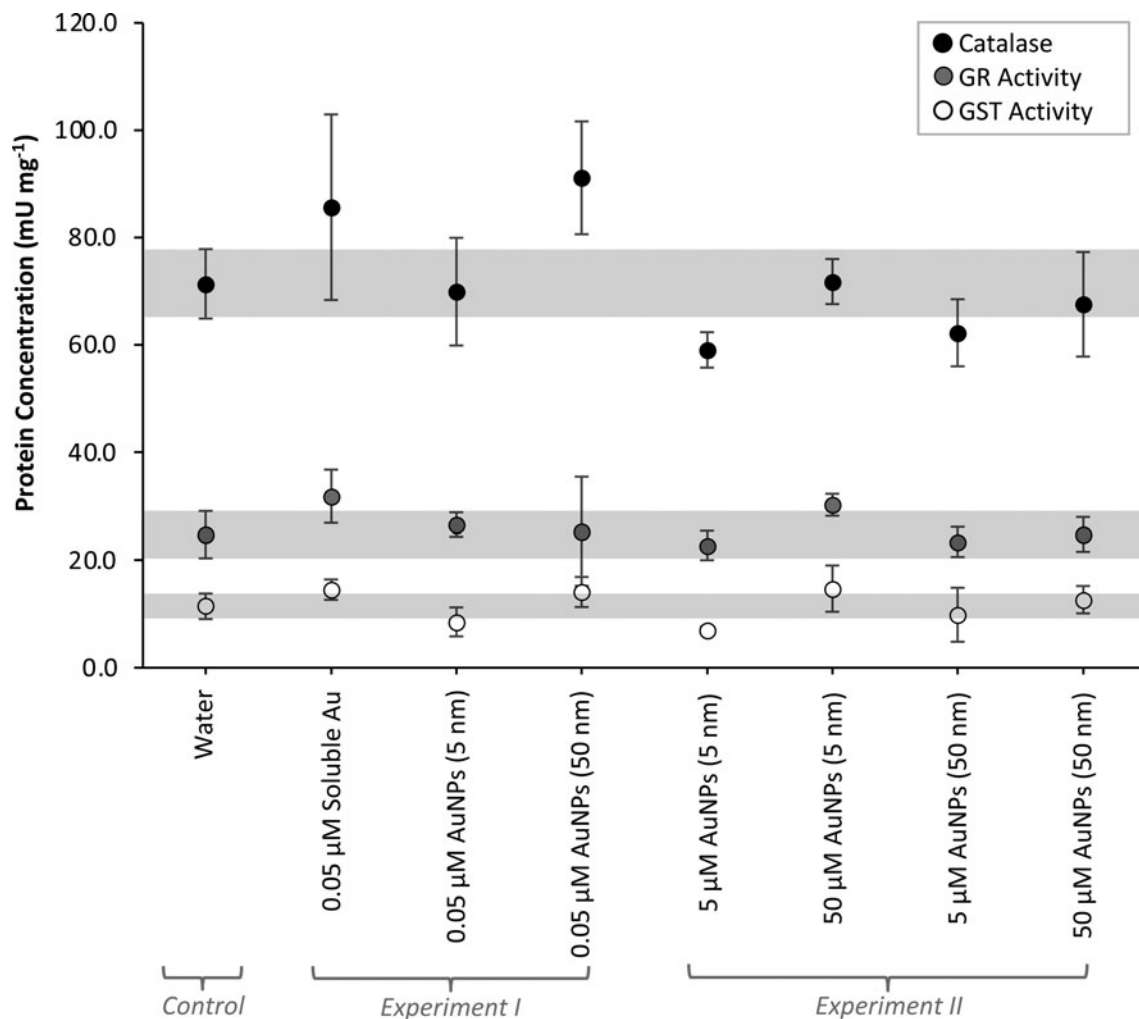


**Fig. 2.** Indicators of stress based on protein concentrations measured from fish larvae using catalase (CAT), glutathione reductase (GR) and glutathione S-transferase (GST) assays.

3 mU mg<sup>-1</sup> relative to the control. Between larvae–gold systems, CAT concentrations from larvae exposed to 0.05 μM aqueous gold or 50 nm AuNPs were similar (Fig. 2, Experiment I).

From Experiment II, larvae exposed to 5 μM of 5 nm AuNPs had average CAT, GR and GST concentrations that were 12, 2 and 4 mU mg<sup>-1</sup> less compared to the control. Larvae exposed to 50 μM of 5 nm AuNPs had an average CAT concentration similar to the control whereas average GR and GST concentrations from this system were 6 and 3 mU mg<sup>-1</sup> greater, respectively, compared to the control. The enzyme assays were similar for larvae that were exposed to 5 or 50 μM concentrations. Larvae exposed to 5 μM of 5 nm AuNPs had average CAT, GR and GST concentrations that were 9, 1 and 2 mU mg<sup>-1</sup> less, respectively, compared to the control. Larvae exposed to 50 μM of 50 nm AuNPs had an average CAT concentration 4 mU mg<sup>-1</sup> less than the control and an average GST concentration 1 mU mg<sup>-1</sup> greater than the control (Fig. 2, Experiment II).

#### Larvae mortality

In terms of total mortality, 10% of fish larvae died in the control after 6 days. All the larvae–gold systems from Experiment I had total mortalities less than the control at the end of the experiment.

Total mortality was the same for larvae exposed to 0.05 μM aqueous Au or 50 nm AuNPs (9%), whereas larvae exposed to 5 nm AuNPs was the lowest (4%). Total mortalities in the larvae–gold systems from Experiment II were higher compared to the control. In general, 5 nm AuNPs appeared to be more lethal than 50 nm AuNPs. Larvae exposed to 5 μM or 50 μM of 50 nm AuNPs had 18% and 19% total mortality, respectively, whereas larvae exposed to 5 μM or 50 μM of 5 nm AuNPs had 23% and 100%, respectively (Fig. 3). It is important to note that the fish larvae–gold system with 100% total mortality occurred after 2 days and were the same fish larvae with ‘swollen’ yolk-sacs.

#### Gold accumulation and distribution within fish larvae

The 0.05 μM AuNPs concentrations used in Experiment I contained  $7.82 \times 10^{12}$  of 5 nm AuNPs and  $7.82 \times 10^9$  of 50 nm AuNPs, respectively, whereas the 50 μM AuNPs concentrations used in Experiment II contained  $7.82 \times 10^{15}$  of 5 nm AuNPs and  $7.82 \times 10^{12}$  50 nm AuNPs. See Table 1 for calculations regarding the number of AuNPs for each concentration. Based on ICP-MS analysis, greater detections of gold within larvae correlated with exposures involving higher concentrations. In terms of moles, larvae exposed to 0.05 μM aqueous gold contained the

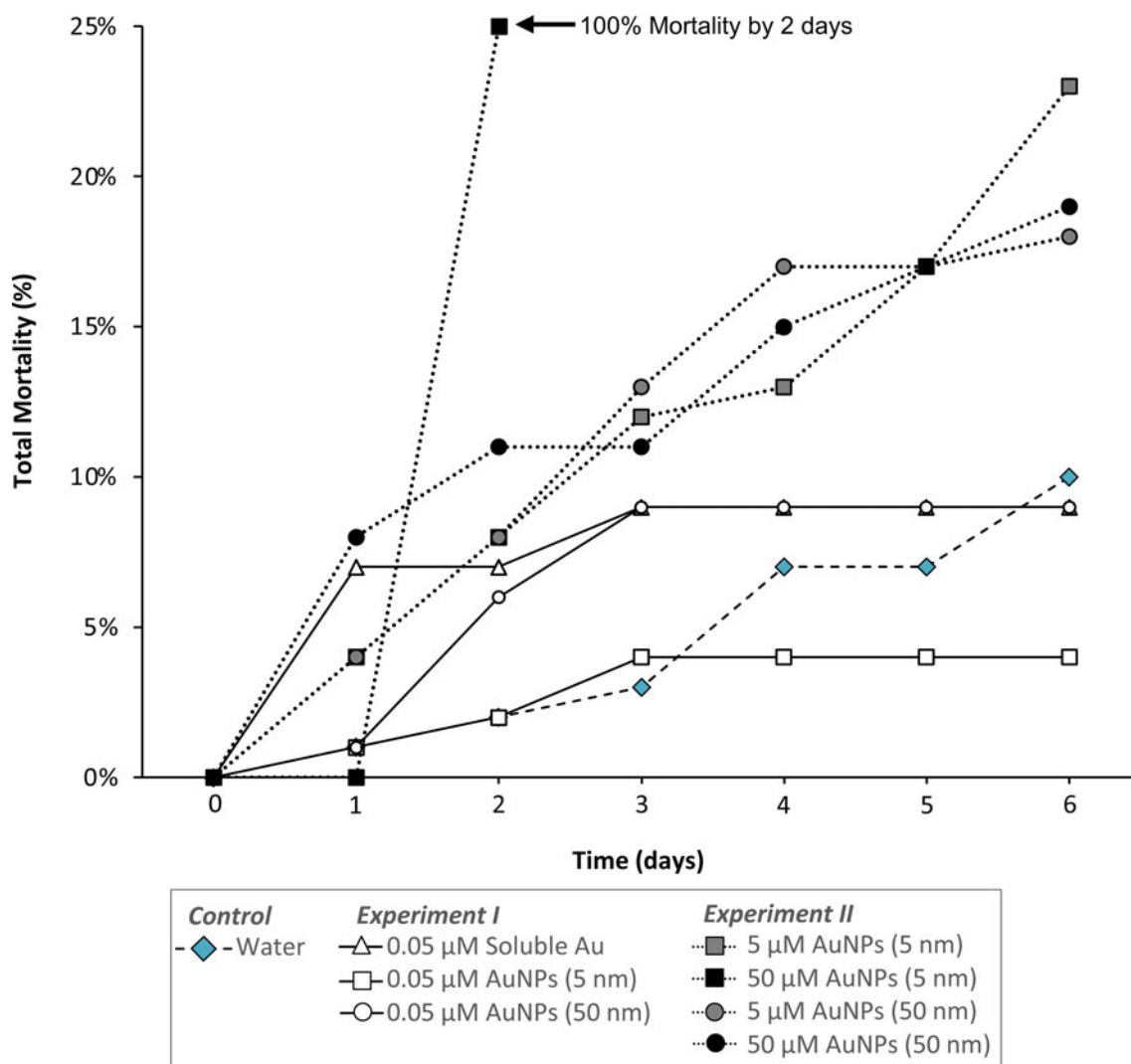


Fig. 3. Total mortality of fish larvae from Experiments I and II and the control over time.

Table 1. Calculations for determining the number of AuNPs in 0.05 and 50 μM concentrations.

AuNP Diameter (nm)	AuNP Volume (nm <sup>3</sup> ) <sup>a</sup>	Unit Cells per AuNP <sup>b</sup>	Au Atoms per AuNP <sup>c</sup>	Au Moles per AuNP <sup>d</sup>	Number of AuNPs in 0.05 μM <sup>e</sup>	Number of AuNPs in 50 μM <sup>f</sup>
5	6.54 × 10 <sup>1</sup>	9.63 × 10 <sup>2</sup>	3.85 × 10 <sup>3</sup>	6.40 × 10 <sup>-21</sup> α	7.82 × 10 <sup>12</sup>	7.82 × 10 <sup>15</sup>
50	6.54 × 10 <sup>4</sup>	9.63 × 10 <sup>5</sup>	3.85 × 10 <sup>6</sup>	6.40 × 10 <sup>-18</sup> β	7.82 × 10 <sup>9</sup>	7.82 × 10 <sup>12</sup>

<sup>a</sup>AuNP Volume = (4/3) π (r<sup>3</sup>). Note that r is half the respective diameter for each AuNP.

<sup>b</sup>Unit cells per AuNP = a ÷ Unit cell of gold (6.79 × 10<sup>-2</sup> nm<sup>3</sup>). Note that gold has a cubic unit cell with a length of 4.08 × 10<sup>-1</sup> nm; hence, the volume is 6.79 × 10<sup>-2</sup> nm<sup>3</sup>.

<sup>c</sup>Au atoms per AuNP = b × 4 atoms per unit cell of gold

<sup>d</sup>Au moles per AuNP = c ÷ Avogadro's number (6.022 × 10<sup>23</sup>).

<sup>e</sup>Number of AuNP = ((0.05 or 50 μM) ÷ (1.0 × 10<sup>6</sup>)) ÷ d.

highest amount of gold (6.24 × 10<sup>-10</sup> moles Au in 10 larvae), which was 25% of aqueous gold removed from solution. Comparatively, larvae exposed to 0.05 μM of 5 or 50 nm AuNPs, removed 8% and 1%, respectively. Larvae exposed to 50 μM of 5 or 50 nm AuNPs, from Experiment II, removed ≤0.1% (Table 2).

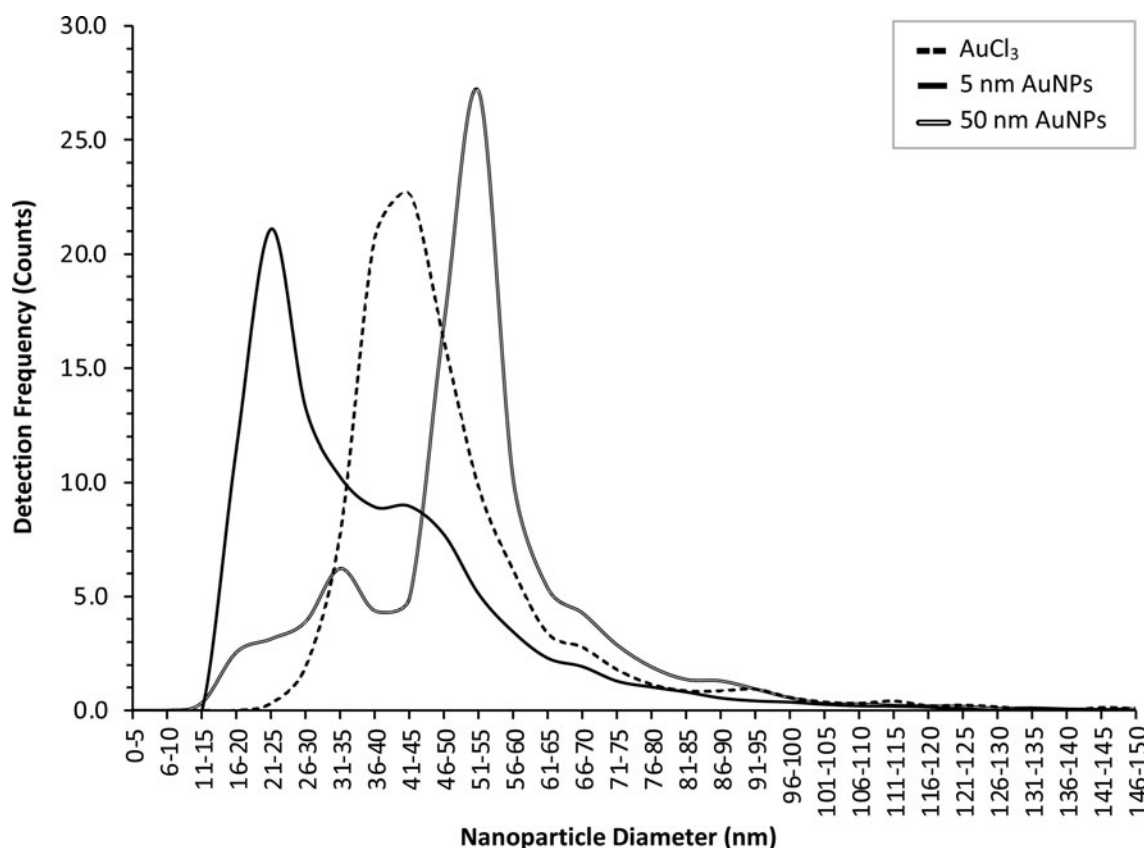
Analysis by SP-ICP-MS indicated that aqueous gold was reduced to elemental AuNPs ranging between 20 to 150 nm in diameter. Though the distribution was somewhat normal, the majority of these nanoparticles were within 41 to 45 nm in size.

The 5 nm AuNPs appeared to form aggregates up to 150 nm in size; however, aggregates between 21 to 25 nm and 41 to 45 nm were most frequent. Similarly, 50 nm AuNPs also formed aggregates that were comparable in size to those comprised of 5 nm AuNPs. In addition to aggregation, the detection of 50 nm AuNPs had a subtle peak indicating smaller nanoparticles with diameters between 31 to 35 nm (Fig. 4).

High-resolution SEM and corresponding EDS confirmed that aqueous gold was reduced as AuNPs within fish larvae. These nanoparticles along with 5 nm AuNPs formed aggregates within

**Table 2.** Calculations for determining the average number of AuNPs within fish larvae from the lowest and highest exposure concentrations.

Experiment	Average Au concentration (mg kg <sup>-1</sup> ) <sup>a</sup>	Au mass per larvae (g) <sup>b</sup>	Au moles per larvae <sup>c</sup>	AuNPs per larvae <sup>d</sup>	Percent gold uptake <sup>e</sup>
Experiment I					
0.05 μM AuCl <sub>4</sub> <sup>*</sup>	1.05 × 10 <sup>1</sup> (±3.25 × 10 <sup>0</sup> )	1.23 × 10 <sup>-8</sup> (±3.81 × 10 <sup>-9</sup> )	6.24 × 10 <sup>-11</sup> (± 1.94 × 10 <sup>-11</sup> )		24.9
0.05 μM AuNPs (5 nm)	3.35 × 10 <sup>0</sup> (±9.70 × 10 <sup>-1</sup> )	3.93 × 10 <sup>-9</sup> (±1.14 × 10 <sup>-9</sup> )	1.99 × 10 <sup>-11</sup> (± 5.78 × 10 <sup>-12</sup> )	3.12 × 10 <sup>9</sup> (±9.03 × 10 <sup>8</sup> ) α	8.0
0.05 μM AuNPs (50 nm)	5.32 × 10 <sup>-1</sup> (±1.25 × 10 <sup>-1</sup> )	6.25 × 10 <sup>-10</sup> (±1.47 × 10 <sup>-10</sup> )	3.17 × 10 <sup>-12</sup> (± 7.44 × 10 <sup>-13</sup> )	4.96 × 10 <sup>5</sup> (±1.16 × 10 <sup>5</sup> ) β	1.3
Experiment II					
50 μM AuNPs (5 nm)	1.68 × 10 <sup>1</sup> (±7.10 × 10 <sup>0</sup> )	1.98 × 10 <sup>-8</sup> (±8.33 × 10 <sup>-9</sup> )	1.00 × 10 <sup>-10</sup> (± 4.23 × 10 <sup>-11</sup> )	1.57 × 10 <sup>10</sup> (±6.61 × 10 <sup>9</sup> ) α	<0.1
50 μM AuNPs (50 nm)	2.48 × 10 <sup>1</sup> (±2.58 × 10 <sup>1</sup> )	2.92 × 10 <sup>-8</sup> (±3.03 × 10 <sup>-8</sup> )	1.48 × 10 <sup>-10</sup> (± 1.54 × 10 <sup>-10</sup> )	2.31 × 10 <sup>7</sup> (±2.40 × 10 <sup>7</sup> ) β	0.1

<sup>a</sup>Au Concentrations measured by ICP-MS<sup>b</sup>Au Mass per Larvae = (a ÷ 1.0 × 10<sup>3</sup>) × average larvae mass (1.17 × 10<sup>-6</sup> kg)<sup>c</sup>Gold Moles per Larvae = b ÷ molar mass of gold (196.96657 g mol<sup>-1</sup>)<sup>d</sup>AuNPs per Larvae = c ÷ (Au moles per AuNP Table 1a)<sup>e</sup>Percent Gold Uptake = (c × 10 larvae) ÷ (Au moles in 50 mL fish larvae-gold system). Note that 0.05 μM is 2.50 × 10<sup>-9</sup> Au mols per 50 mL and 50 μM is 2.50 × 10<sup>-6</sup> Au mols per 50 mL.<sup>\*</sup>Reduction of soluble gold resulted in a range of AuNP sizes. See Fig. 4.**Fig. 4.** Size distribution of AuNPs within fish larvae. Note that detection frequencies are the sum of the two concentrations (0.05 and 50 μM) for each respective AuNPs size.

cells comprising the epidermis and fin. Aggregated AuNPs appeared to form larger clusters up to 1 μm in size (Fig. 5). Note that 50 nm AuNPs were not observed within cells of the epidermis or fin. A summary of all larvae-gold systems and the different analytical techniques can be found in Table 3.

## Discussion

### Gold-induced stress and the toxicity of AuNPs

The lipophilicity of yolk-sacs prevents solutes from permeating the internal environment; however, some compounds can passively enter cells comprising the yolk-sac (Sant and

Timme-Laragy, 2018). For example, nanoparticulate materials, such as ZnO and SiO<sub>2</sub>, have been shown to cause yolk-sac edema (swelling) in zebrafish embryos (Choi *et al.*, 2016; Chao *et al.*, 2017). Similarly, silver nanoparticles have been known to cause edema and physical abnormalities, as well as disrupting gill osmoregulation (Wu *et al.*, 2010; Masouleh *et al.*, 2017). In this study, 5 nm AuNPs caused the greatest swelling of yolk-sacs (Fig. 1). Gold nanoparticles <10 nm in diameter can pass directly through cell membranes (Jiang *et al.*, 2015). Therefore, it is reasonable to suggest that both aqueous gold and the 5 nm AuNPs passively entered into the larvae. The latter form of gold, at higher concentrations, resulted in the most extensive yolk-sac edema, consequently impacting the larvae's notochords. The 50 nm

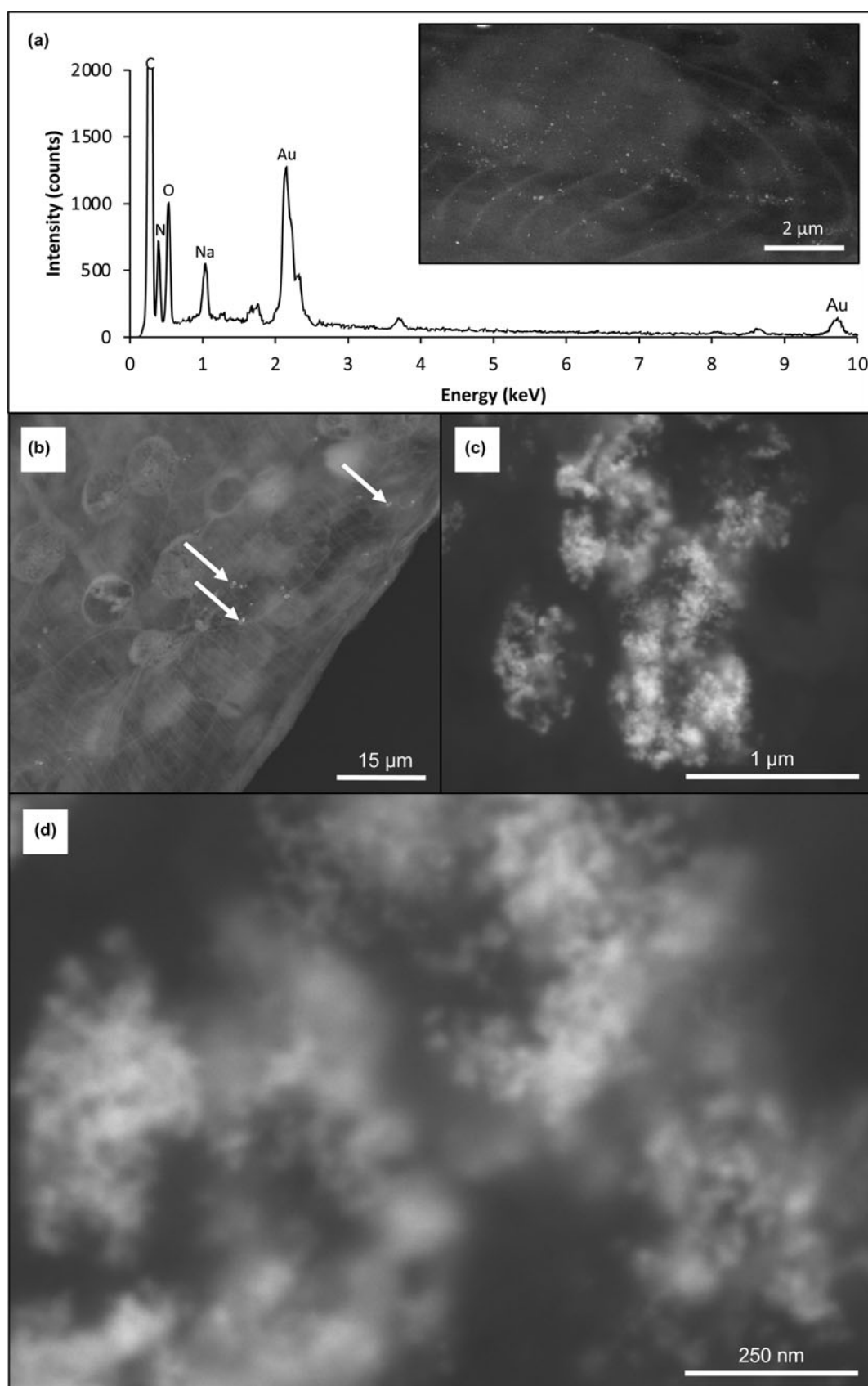


**Fig. 5.** (a) A representative energy-dispersive spectrum confirming that aqueous gold was reduced to elemental AuNPs within fish larvae; (inset) a corresponding low-magnification back-scatter electron (BSE) micrograph of fin cells containing reduced aqueous gold. (b) A low-magnification BSE-SEM micrograph of 5 nm AuNPs aggregated (arrows) within cells of a dorsal fin. (c) A high-magnification BSE-SEM micrograph of an aggregated 5 nm AuNPs in epidermis cells. (d) The aggregates appear to form a larger cluster.



**Table 3.** A summary of larvae–gold systems (i.e. treatment) and the number of larvae used for each analysis.

Analysis	Control	Experiment I (3 larvae–gold systems) *			Experiment II (4 larvae–gold systems) *			
		0.05 $\mu\text{M}$ $\text{AuCl}_3$	0.05 $\mu\text{M}$ AuNPs (5 nm)	0.05 $\mu\text{M}$ AuNPs (50 nm)	5 $\mu\text{M}$ AuNPs (5 nm)	50 $\mu\text{M}$ AuNPs (5 nm)	5 $\mu\text{M}$ AuNPs (50 nm)	50 $\mu\text{M}$ AuNPs (50 nm)
Yolk-sac measurement (i.e. Fig. 1) **	10	10	10	10	10	10	10	10
CAT, GR, GST Activity (i.e. Fig. 2)	5	5	5	5	5	5	5	5
Total mortality (i.e. Fig. 3)	10	9	4	9	23	100	18	19
SP-ICP-MS (i.e. Fig. 4)	1	1	1	1		1		1
SEM-EDS (i.e. Fig. 5) **	10	10	10	10	10	10	10	10
ICP-MS (i.e. Table 1)	3	3	3	3		3		3

\*Each larvae–gold system involved 100 larvae.

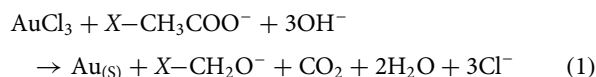
\*\*These were the same larvae.

AuNPs were too large to passively enter cells, which would explain the lack of detection using SEM. However, detection based on SP-ICP-MS and ICP-MS suggests that these particles could have been taken up through the mouth or gills. It is possible that the uptake of these AuNPs via the gills could have disrupted osmoregulation thereby resulting in yolk-sac swelling. From a biochemical perspective, the majority of larvae exposed to gold did not express high enzymatic activity (CAT, GR activity or GST activity) relative to the control. Golden perch are known to quickly acclimatise and recover from stress ranging from chronic to acute levels (Carragher and Rees, 1994). Therefore, it can be interpreted that these larvae were actively acclimating to the presence of gold within the respective larvae–gold systems (Fig. 2). It is important to note that larvae exposed to aqueous gold expressed greater oxidative stress compared to the controls. Gold complexes, like other heavy metals, exert an oxidative stress on cells and have a strong affinity for sulfur-bearing compounds such as thiol (HS) functional groups in glutathione (Ortego *et al.*, 2014). The increased concentration of GR and GST in larvae exposed to aqueous gold could also suggest that cells were trying to replenish these S-bearing compounds that were ‘lost’ to aqueous gold. Additionally, this provides a possible mechanism for gold nanoparticle formation within cells, which was observed by SEM (biomineralisation discussed below). Overall, the ability of larvae to acclimate to stress is reflected in the low mortality rates where at least 75% of the entire population survived after 7 days (Fig. 3). From Experiment I, larvae mortality was similar yet more gold was detected within larvae exposed to aqueous gold compared to AuNPs, supporting the notion that solutes and particles <10 nm can cross cell walls/membranes (Table 1; Jiang *et al.*, 2015). Of the all the larvae–gold systems, the 50  $\mu\text{M}$  concentration of 5 nm AuNPs (from Experiment II) was the most lethal and the amount of gold detected within these larvae represented <1% of the exposure concentrations. The rate of uptake of AuNPs was probably a sudden shock to the larvae hence the limited expression of stress (proteins) prior to death.

#### Gold mineralisation and AuNPs accumulation

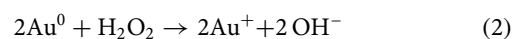
The reduction of aqueous gold complexes, by organic compounds, generally produces a relatively normal distribution of nanoparticle sizes (Turkevich *et al.*, 1951). Since this early study, various types of organic materials (bacteria, fungi and other chemicals) have been shown to reduce aqueous gold, forming nanoparticles (Shuster and Reith, 2018; Bohu *et al.*, 2019; Daruich De Souza *et al.*, 2019 and references therein). For

example, aqueous gold can be reduced by fatty acid, a model organic compound, contributing to mineralisation, Reaction 1:



Additionally, the presence of heavy metals is known to increase the production of glutathione (Lu, 2009; Townsend *et al.*, 2003). In this study, aqueous gold was reduced as AuNPs with the majority occurring between 21–25 nm in diameter. It is reasonable to suggest that aqueous gold could have been binding with glutathione and could explain the increased enzymatic activity. Interestingly, these AuNPs did not appear to ‘coat’ the larvae indicating that the aqueous complex entered cells passively and biomineralisation occurred intracellularly, primarily with epidermis and fin cells that were in direct contact with water (Figs 3–5). Additionally, glutathione can serve as a molecular linker for AuNPs (Basu and Pal, 2007; Chen *et al.*, 2012). The clustering of these AuNPs, including larvae exposed to 5 nm AuNPs, not only highlights the cellular uptake of gold but also its transport within cells, which is dependent on nanoparticle size (Liu *et al.*, 2017). This could also be important for AuNPs ‘transformation’ (dissolution and re-precipitation) within a cellular environment.

In regard to exposures to different size AuNPs, the ‘peak’ and ‘shoulder’ at 21–25 nm and 45–50 nm, respectively, could be attributed to aggregation of 5 nm AuNPs (Kim *et al.*, 2008) after extraction from larvae. On the contrary, the small peak at 31–35 nm for the 50 nm AuNPs could suggest that these nanoparticles were reduced in size within larvae prior to extraction. Cells produce hydrogen peroxide, a reactive oxygen species (ROS), as a stress response to contaminants such as heavy metals; hence the production of catalase to release oxygen from hydrogen peroxide subsequently reducing the concentration of this ROS (Schieber and Chandel, 2014; Holmström and Finkel, 2014). Inferred from increased catalase production, it is possible that hydrogen peroxide could have been a biochemical mechanism for AuNPs dissolution leading to smaller nanoparticle sizes (Reaction 2):



Intuitively, solubilised gold would probably not remain stable and would, therefore, become reduced as smaller AuNPs (Fig. 4).

### Implications for future ecotoxicological studies

*In vitro* experiments demonstrated that AuNPs are mobile within water columns, accumulate in the food web and therefore have the potential for similar mobility within natural environments (Ferry *et al.*, 2009). In light of this potential, measurable amounts of gold have been detected in wastewater treatment plants from communities with strong industrial activities related to mining, metal refining and jewellery production (Reeves *et al.*, 1999; Westerhoff *et al.*, 2015; Vriens *et al.*, 2017). With increased AuNPs used in electronic and pharmaceutical applications, it is reasonable to suggest that gold from wastewater, if left untreated, will make its way back to the natural environment. This phenomenon has been observed with silver nanoparticles from commercial products (Lombi *et al.*, 2013). Although AuNPs are considered generally to be low-risk in terms of toxicity (Alkilany *et al.*, 2010), the detection in wastewaters further highlights its social value and the need to steer future behaviours. The more that is known about AuNPs and their interaction with various organisms, the more prepared society will be to deal with environmental contamination.

The results from this present study broadly highlights the effects of gold on golden perch larvae. While this study provides information in regard to relative stress tolerance, future studies could involve golden perch at different growth stages (embryos or adult), a range of AuNPs sizes <10 nm, or different nanoparticle compositions (e.g. gold–silver alloy). Additionally, to prevent AuNPs from naturally aggregating, ligands such as citrate or alkanethiols are used as ‘capping’ agents (Frens 1973; Brust *et al.*, 1994). Depending on the amount of capping agent per nanoparticle, the concentration of ligands can be more toxic than the nanoparticles themselves (Ju-Nam and Lead, 2008; Chen *et al.*, 2009; Perala and Kumar, 2013). Therefore, future studies could assess how ligands on ‘spent’ AuNPs (nanoparticles used for initial biomedical or technological purposes) could impact larvae and fish. Indeed, the increasing use of AuNPs and the potential for contamination in natural environments has been the incentive for assessing their effect on various organisms (e.g. Chen *et al.*, 2009; Zhang *et al.*, 2019 and references therein). Because AuNPs can adsorb to both organic and inorganic materials (Hanlie *et al.*, 2006; Zhu *et al.*, 2009; Feichtmeier *et al.*, 2015), the occurrence of AuNPs in natural environments requires assessment to accurately determine ‘environmentally relevant’ concentrations that actually pose risks. Additionally, the chemistry of different natural water systems (wastewater, lakes and rivers) could influence the structure or chemistry of AuNPs or gold-alloy nanoparticles. Therefore, future studies could investigate how water chemistry could influence the toxicity of AuNPs using experimental systems (microcosms) that are more representative of natural environmental conditions. Dynamic modelling of AuNPs mobility within these environments would also complement future ecotoxicological studies to understand how uptake of dispersed AuNPs could differ from monodispersed AuNPs.

### Conclusion

In this study, golden perch (*Macquaria ambigua*) larvae were exposed to gold for up to 6 days. The effect of gold was based on larval responses to aqueous gold, 5 nm AuNPs, or 50 nm AuNPs (Experiment I). Similarly, the relationship between AuNPs dosages and larval responses was also assessed (Experiment II). Overall, aqueous gold and 5 nm AuNPs are

capable of entering epidermis and fin cells that are in direct contact to gold-bearing water, whereas 50 nm AuNPs were probably ingested. Both uptake mechanisms appear to have caused yolk-sac swelling with variable expression of oxidative stress enzymes. Though higher concentrations of smaller AuNPs were most lethal, the mortality within the other larvae–gold systems was comparable to the control suggesting that a fraction of the population would have been able to continue developing into adult fish. As a model, this study highlighted how larvae tolerate, or could acclimatise, to the presence of aqueous gold or AuNPs derived from anthropogenic use (biomedical and technological applications) that are not recovered from wastewater treatment. Additionally, this model could provide some insight on the tandem effects of alloy nanoparticles. Indeed, the extent of yolk-sac swelling, expression of stress proteins, and mortality rate would vary under *in situ* conditions, especially as biogeochemical processes could alter AuNPs structure as well as the chemistry of the coating, if present. In conclusion, this study provides a broad perspective of how fish larvae could be impacted by aqueous gold and AuNPs. The use of AuNPs in biomedical and electronic application continues to increase and diversify, which could inadvertently contaminate natural environments. Therefore, the potential for AuNPs to contaminate natural water systems is the motivation for assessing the effect of AuNPs on golden perch.

**Acknowledgements.** This research was based on the CSIRO AEC Project 817 and supported, in part, by the Australian Research Council (ARC) Future Fellowship (FT100150200) awarded to the late Frank Reith (c/o Jeremiah Shuster). Experiments and enzyme activity assays were performed at CSIRO Land and Water, Environmental Toxicology and Chemistry (Urrbrae, SA 5064, Australia). Scanning electron microscopy analysis was performed at Adelaide Microscopy, The University of Adelaide (Adelaide, SA 5005, Australia). Single-particle inductively coupled plasma mass spectroscopy analysis was performed at Flinders Analytical, Flinders University (Bedford Park, SA 5042, Australia). Inductively coupled plasma mass spectroscopy analysis was performed at CSIRO Analytical Services Unit (Urrbrae, SA 5064, Australia). We thank Hapreet Bhatia, Animesh Basak, Jason Young, John Gouzos and Claire Wright for their technical support.

### References

- Aebi H. (1984) Catalase. *Methods in Enzymology*, **105**, 121–126.
- Alkilany A.M. and Murphy C.J. (2010) Toxicity and cellular uptake of gold nanoparticles: What we have learned so far? *Journal of Nanoparticle Research*, **12**, 2313–2333.
- Basu S. and Pal T. (2007) Glutathione-induced aggregation of gold nanoparticles: electromagnetism interactions in a closely packed assembly. *Journal of Nanoscience and Nanotechnology*, **7**, 1904–1910.
- Bhagyaraj S. M. and Oluwafemi O.S. (2018) Nanotechnology: The science of the invisible. Pp. 1–18 in: *Micro and Nano Technologies – Synthesis of Inorganic Nanomaterials* (S.M. Bhagyaraj, S.O. Oluwatobi, N. Kalarikkal and S. Thomas, editors). Woodhead Publishing, Cambridge, UK.
- Bohu T., Anand R., Noble R., Lintern M., Kaksonen A.H., Mei Y., Cheng K.Y., Deng X., Veder J., Bunce M., Power M. and Verral M. (2019) Evidence for fungi and gold redox interaction under Earth surface conditions. *Nature Communications*, **10**, 2290.
- Bradford M.M. (1976) A rapid and sensitive method for the quantification of microgram quantities of protein utilizing the principle of protein-dye binding. *Analytical Biochemistry*, **72**, 248–254.
- Brust M., Walker M., Bethell D., Schiffrin D.J. and Whyman R.J. (1994) Synthesis of thio derivatised gold nanoparticles in a two-phase liquid/liquid system. *Journal of the Chemical Society, Chemical Communications*, **7**, 801–802.
- Carragher J.F. and Rees, C.M. (1994) Primary and secondary stress responses in golden perch, *Macquaria ambigua*. *Comparative Biochemistry and Physiology*, **107A**, 49–56.

- Chao S.J., Huang C.P., Chen P.C. and Huang C. (2017) Teratogenic responses of zebrafish embryos to decabromodiphenyl ether (BDE-209) in the presence of nano-SiO<sub>2</sub> particles. *Chemosphere*, **178**, 449–457.
- Choi J.S., Kim R.O., Yoon S. and Kim W.K. (2016) Developmental toxicity of zinc oxide nanoparticles to zebrafish (*Danio rerio*): A transcriptomic analysis. *PLoS ONE*, **11**, e0160763, <https://doi.org/10.1371/journal.pone.0160763>
- Chen Y.S., Hung Y.C., Lian I. and Huang G.S. (2009) Assessment of the in-vitro toxicity of gold nanoparticles. *Nanoscale Research Letters*, **4**, 858–864.
- Chen X., Li Q.W. and Wang X.M. (2014) Gold nanostructures for bioimaging, drug delivery and therapeutics. Pp. 163–176 in: *Precious Metals for Biomedical Applications* (N. Baltzer and T. Copponnex, editors). Woodhead Publishing, Cambridge, UK.
- Chen Z., Wang Z., Chen J., Wang S. and Huang X. (2012) Sensitive and selective detection of glutathione based on resonance light scattering using sensitive gold nanoparticles as colorimetric probes, *Analyst*, **137**, 3132–3137.
- Daruich De Souza C., Nogueira B.R., Elisa M. and Rostelato C.M. (2019) Review of the methodologies used in the synthesis gold nanoparticles by chemical reduction. *Journal of Alloys and Compounds*, **798**, 714–740.
- Drotar A., Phelps P. and Fall R. (1985) Evidence for glutathione peroxidase activities in cultured plant cells. *Plant Science*, **42**, 35–40.
- Dykman L.A. and Khlebtsov N.G. (2011) Gold nanoparticles in biology and medicine: Recent advances and prospects. *Acta Naturae*, **3**, 34–55.
- Feichtmeier N.S., Walther P. and Leopold K. (2015) Uptake, effect, and regeneration of barley plant exposed to gold nanoparticles. *Environmental Science and Pollution Research*, **22**, 8549–8558.
- Ferry J.L., Craig P., Hexel C., Sisco P., Frey R., Pennington P.L., Fulton M.H., Scott I.G., Decho A.W., Kashiwada S., Murphy C.J. and Shaw T.J. (2009) Transfer of gold nanoparticles from the water column to the estuarine food web. *Nature Nanotechnology*, **4**, 441–444.
- Frens G. (1973) Controlled nucleation for the regulation of the particle size in monodispersed gold suspensions. *Nature Physical Science*, **241**, 20–22.
- Hanlie H., Liyun T., Qiujuan B. and Yong Z. (2006) Interface characteristics between colloidal gold and kaolinite surface by XPS. *Journal of Wuhan University of Technology – Material Science Edition*, **21**, 90–93.
- Harris J.H. and Rowland S.J. (1996) Family Percichthyidae: Australian freshwater cods and basses. Pp. 150–163 in: *Freshwater Fishes of South-Eastern Australia*. (R.M. McDowall, editor). Reed, Chatswood, NSW, Australia.
- Holmström K.M. and Finkel T. (2014) Cellular mechanisms and physiological consequences of redox-dependent signalling. *Nature Reviews Molecular Cell Biology*, **15**, 411–421.
- Jiang Y., Huo S., Mizuhara T., Das R., Lee Y., Hou S., Moyano D.F., Duncan B.D., Liang X. and Rotello V.M. (2015) The interplay of size and surface functionality on the cellular uptake of sub-10 nm gold nanoparticles. *ACS Nano*, **9**, 9986–9993.
- Ju-Nam Y. and Lead J.R. (2008) Manufactured nanoparticles: An overview of their chemistry, interactions and potential environmental implications. *Science of the Total Environment*, **400**, 396–414.
- Khaksar M., Jolley D.F., Sekine R., Vasilev K., Johannessen B., Donner E. and Lombi E. (2015) In situ chemical transformation of silver nanoparticles along the water-sediment continuum. *Environmental Science & Technology*, **49**, 318–325.
- Kim T., Lee C., Joo S. and Lee K. (2008) Kinetics of gold nanoparticle aggregation: Experiments and modelling. *Journal of Colloidal and Interface Science*, **318**, 238–243.
- Liu M., Li Q., Liang L., Li J., Wang K., Li J., Lv M., Chen N., Song H., Lee J., Shi J., Wang L., Lal R. and Fan C. (2017) Real-time visualization of clustering and intracellular transport of gold nanoparticles by correlative imaging. *Nature Communications*, **8**, 15646.
- Lombi E., Donner E., Taheri S., Tavakkoli E., Jamting A.K., McClure S., Naidu R., Miller B.W., Scheckel K.G. and Vasilev K. (2013) Transformation of silver/silver chloride nanoparticles during anaerobic treatment of wastewater and post-processing of sewage sludge. *Environmental Pollution*, **176**, 193–197.
- Lu S.C. (2009) Regulation of glutathione synthesis. *Molecular Aspects of Medicine*, **30**, 42–59.
- Mallen-Cooper M., Stuart I.G., Hides-Pearson F. and Harris J.H. (1995) *Migration in the Murray River and Assessment of the Torrumbarry Fishway. Final Report for Natural Resources Management Strategy Project N002*. NSW Fisheries and CRC for Freshwater Ecology, Cronulla, NSW, Australia.
- Masouleh F.F., Amiri B.M., Mirvaghefi A., Ghafoori H. and Madsen S.S. (2017) Silver nanoparticles cause osmoregulatory impairment and oxidative stress in Caspian kutum (*Rutilus kutum*, Kamensky 1901). *Environmental Monitoring and Assessment*, **189**, 1–12.
- Ortego L., Cardoso F., Martins S., Fillat M.F., Laguna A., Meireles M., Villacampa M.D. and Concepción Gimeno M. (2014) Strong inhibition of thioredoxin reductase by highly cytotoxic gold(I) complexes. DNA binding study. *Journal of Inorganic Biochemistry*, **130**, 32–37.
- Perala S.R.K. and Kumar S. (2013) On the mechanism of metal nanoparticle synthesis in the Brust-Schiffrin method. *Langmuir*, **29**, 9863–9873.
- Rea M.A., Shuster J., Kumar A., Reith F. and Stephan C. (2020) extraction of gold nanoparticles from fish larvae and soils. *PerkinElmer Application Notes*, 1–5.
- Reeves S.J., Plimer I.R. and Foster D. (1999) Exploitation of gold in historic sewage sludge stockpile, Werribee, Australia: Resource evaluation, chemical extraction and subsequent utilization of sludge. *Journal of Geochemical Exploration*, **65**, 141–153.
- Reith F., Brugger J., Zammit C., Nies D.H. and Southam G. (2013) Geobiological cycling of gold: From fundamental process understanding to exploration solutions. *Minerals*, **3**, 367–394.
- Reynolds L.F. (1983) Migration patterns of five fish species in the Murray-Darling river system. *Australian Journal of Marine and Freshwater Research*, **34**, 857–871.
- Sant K.E. and Timme-laragy A.R. (2018) Zebrafish as a model for toxicological perturbation of yolk and nutrition in the early embryo. *Current Environmental Health Reports*, **5**, 125–133.
- Schieber M. and Chandel N.S. (2014) ROS function in redox signalling and oxidative stress. *Current Biology*, **10**, R453–R462.
- Shuster J. and Reith F. (2018) Reflecting on gold geomicrobiology research: Thoughts and considerations for future endeavours. *Minerals*, **8**, 1–12.
- Shuster J., Reith F., Cornelis G., Parsons J.E., Parsons J.M. and Southam G. (2017) Secondary gold structures: Relics of past biogeochemical transformations and implications for colloidal gold dispersion in subtropical environments. *Chemical Geology*, **450**, 154–164.
- Shuster J., Southam G. and Reith F. (2019) Applications of scanning electron microscopy in geomicrobiology. Pp. 148–165 in: *Analytical Geomicrobiology: A Handbook of Instrumental Techniques* (J.P.L. Kenney, H. Veeramani and D. Alessi, editors). Cambridge University Press, Cambridge, UK.
- Smith I.K., Vierheller T.L. and Thorne C.A. (1988) Assay of glutathione reductase in crude tissue homogenates using 5,5'-dithiobis(2-nitrobenzoic acid). *Analytical Biochemistry*, **175**, 408–413.
- Townsend D.M., Tew K.D. and Tapiero H. (2003) The importance of glutathione in human disease. *Biomedicine and Pharmacotherapy*, **57**, 145–155.
- Turkevich J., Stevenson P.C. and Hillier J. (1951) A study of the nucleation and growth processes in the synthesis of colloidal gold. *Discussion of the Faraday Society*, **11**, 55–75.
- Vriens B., Voegelin A., Hug S.J., Kaegi R., Winkel L.H.E., Buser A.M. and Berg M. (2017) Quantification of element fluxes in wastewaters: A nationwide survey in Switzerland. *Environmental Science & Technology*, **51**, 10943–10953.
- Westerhoff P., Lee S., Yang Y., Gordon G.W., Hristovski K., Halden R.U. and Herckes P. (2015) Characterisation, recovery opportunities and valuation of metals in municipal sludge from U.S. wastewater treatment plants nationwide. *Environmental Science & Technology*, **49**, 9479–9488.
- Wu Y., Zhou G., Li H., Liu W., Wang T. and Jiang G. (2010) Effect of silver nanoparticles on the development and histopathology biomarkers of Japanese medaka (*Oryzias latipes*) using the partial-life test. *Aquatic Toxicology*, **100**, 160–167.
- Zhang M., Yang J., Cai Z., Feng Y., Wang Y., Zhang D. and Pan X. (2019) Detection of engineered nanoparticles in aquatic environments: Current status and challenges in enrichment, separation, and analysis. *Environmental Science Nano*, **6**, 709.
- Zhu L., Letaief F., Liu Y., Gervais F. and Detellier F. (2009) Clay mineral-supported gold nanoparticles. *Applied Clay Science*, **43**, 439–446.